ISSN 0915-633X

NATIONAL INSTITUTE FOR FUSION SCIENCE

Pair Annihilation Effects on Surface Ion Cyclotron Wave in Semi-bounded Electron-positron-ion Plasmas

Young-Dae Jung and Daiji Kato

(Received - July 18, 2008)

NIFS-887 Aug. 2008

RESEARCH REPORT
NIFS Series

TOKI, JAPAN

Pair annihilation effects on surface ion cyclotron wave in semi-bounded electron-positron-ion plasmas

Young-Dae Jung[a)]
National Institute for Fusion Science, Toki, Gifu, 509-5292, Japan and Department of Applied Physics, Hanyang University, Ansan, Kyunggi-Do 426-791, South Korea

Daiji Kato
National Institute for Fusion Science, Toki, Gifu, 509-5292, Japan

The electron-positron pair annihilation effects on the surface ion cyclotron wave are investigated in magnetized electron-positron-ion plasmas in atmospheres of neutron stars. The dispersion relation of the surface ion cyclotron wave is obtained by the specular reflection boundary condition with the plasma dielectric function. It is shown that the high- and low-frequency modes of the surface ion cyclotron wave could be existed in electron-positron-ion plasmas. For the high-frequency mode, the pair annihilation enhances the wave frequency in large wave number domains. However, the pair annihilation effects are found to be negligible for the low-frequency mode. It is also found that an increase of the electron temperature or a decrease of the positron temperature strongly suppresses the wave frequency. It is shown that an increase of the magnetic field strongly enhances the wave frequency.

Keywords: pair annihilation, surface wave, electron-positron-ion plasmas

[a)]Permanent address: Department of Applied Physics, Hanyang University, Ansan, Kyunggi-Do 426-791, South Korea. Electronic mail: ydjung@hanyang.ac.kr

PACS number; 52.20.-j

I. INTRODUCTION

The investigation of the surface waves[1-3] in plasmas has been of a great interest since their spectral frequency spectra provide useful information on plasma parameters for spatially bounded plasmas. The electron-positron-ion plasmas have been encountered in various astrophysical environments such as active galactic nuclei, atmosphere of neutron stars, pulsar magnetospheres, and supernova environments.[4] In these astrophysical environments, the direct and indirect positron annihilations with electrons are now of great interests and have been extensively investigated.[5,6] Recently, the propagation of plasma waves has been extensively investigated in electron-positron pair plasmas.[7-12] However, to the best of our knowledge, the electron-positron pair annihilation effects on the surface ion cyclotron wave in magnetized electron-positron-ion plasmas have not been investigated as yet. The theoretical investigation on the dispersion properties of the surface wave in electron-positron-ion plasmas can be a useful tool for investigating the structure and physical properties of electron-positron-ion plasmas. Thus in this paper, we investigate the pair annihilation effects on the propagation of the surface ion cyclotron wave along the plasma-vacuum interface in magnetized electron-positron-ion plasmas. The specular reflection analysis[1] is employed to investigate the plasma dispersion relation since it has been known that the specular reflection condition is quite useful to investigate the dispersion properties of surface waves propagating on the plasma-vacuum interface.

This paper is composed as follows. In Sec. 2 we discuss the specular reflection condition for the surface wave propagating along the plasma-vacuum interface with the plasma dielectric function in magnetized electron-positron-ion plasmas. In Sec. 3, we obtain the dispersion relation of the surface ion cyclotron wave in atmospheres of neutron stars. We also obtain the group velocities for the high- and low-frequency modes of the surface ion cyclotron wave. In Sec. 4, we discuss the electron-positron pair annihilation effects on the wave frequency and the group velocity of the surface ion cyclotron wave. Finally, the conclusions are given in Sec. 5.

II. SPECULAR REFLECTION CONDITION

The specular reflection condition is known to be particularly useful to investigate the dispersion properties of various surface waves in plasmas. The dispersion relation for surface electromagnetic waves propagating in the *z*-direction with the plasma-vacuum interface at $x=0$ can be obtained by the specular reflection condition[1] determined by the surface impedances:

$$\sqrt{\frac{k_z^2c^2}{\omega^2}-1}+\frac{\omega}{\pi c}\int_{-\infty}^{\infty}\frac{dk_x}{k^2}\left[\frac{k_z^2c^2}{\omega^2\varepsilon_l(\omega,k)}-\frac{k_x^2c^2}{k^2c^2-\omega^2\varepsilon_t(\omega,k)}\right]=0\,, \qquad (1)$$

where $\varepsilon_l(\omega,k)$ and $\varepsilon_t(\omega,k)$ are the longitudinal and transverse components of the plasma dielectric function, ω is the frequency, c is the speed of the light, and $k(=\sqrt{k_x^2+k_z^2})$ is the wave number. In this geometry, the *y*-coordinate can be ignored without loss of generality since the *y*-coordinate is a translational invariance. For surface electrostatic waves, i.e., the quasi-static limit $(\omega^2\varepsilon/c^2<<k^2)$, the specular reflection condition for the electrostatic wave propagating along the *z*-direction would be expressed as

$$\frac{1}{\pi}\int_{-\infty}^{\infty}\frac{dk_x\,k_z}{k^2\,\varepsilon_l(\omega,k_x,k_z)}+1=0. \qquad (2)$$

It is well known that the physical properties of electrostatic waves in plasmas would be resolved by the plasma dielectric function. In magnetized electron-positron-ion plasmas, the plasma dielectric function is represented by the summation of the dielectric susceptibilities $\chi_\alpha\ (\alpha=-,+,i)$ of electrons (e^-), positrons (e^+), and ions (*i*):

$$\varepsilon_l(\omega,k)=1+\chi_-+\chi_++\chi_i\,. \qquad (3)$$

The dielectric susceptibility[13] of the species α in magnetized thermal plasmas is written in integral form as

$$\chi_\alpha = \frac{\omega_{p\alpha}^2}{k^2 v_{T\alpha}^2}\left[1-\omega\sum_{l=-\infty}^{\infty} I_l(k_x^2 v_{T\alpha}^2/\omega_{c\alpha}^2)\exp(-k_x^2 v_{T\alpha}^2/\omega_{c\alpha}^2)\int_{-\infty}^{\infty}\frac{dv_z f_\alpha(v_z)}{\omega-k_z v_z - l\omega_{c\alpha}}\right], \tag{4}$$

where $\omega_{p\alpha}(=\sqrt{4\pi n_\alpha q_\alpha^2/m_\alpha})$ is the plasma frequency of the species α, n_α is the density of the species α without the electron-positron pair annihilations, q_α is the charge, m_α is the mass, $v_{T\alpha}(=\sqrt{k_B T_\alpha/m_\alpha})$ is the thermal velocity, k_B is the Boltzmann constant, T_α is the plasma temperature, I_l is the modified Bessel function of order *l*, $\omega_{c\alpha}(=|q_\alpha|B/m_\alpha c)$ is the cyclotron frequency, *B* is the strength of the magnetic field, and $f_\alpha(v_z)[=(2\pi v_{T\alpha}^2)^{-1/2}\exp(-v_z^2/2v_{T\alpha}^2)]$ is the Maxwellian distribution function. In the range of the ion plasma wave, $kv_{Ti} << \omega << k_z v_{Te}, \omega_{ce}k_z/k_x$, $kv_{T\alpha} << \omega_{c\alpha}$, the dielectric susceptibilities for electrons $(-)$, positrons $(+)$, and ions (i) including the electron-positron pair annihilations are, respectively, found to be

$$\chi_- \approx \frac{1}{k^2\lambda_{D_-}^2}\left(1-\frac{n_+}{n_-}\delta\right), \tag{5}$$

$$\chi_+ \approx \frac{1}{k^2\lambda_{D_+}^2}(1-\delta), \tag{6}$$

$$\chi_i \approx -\frac{\omega_{pi}^2 k_\perp^2}{(\omega^2-\omega_{ci}^2)k^2} - \frac{\omega_{pi}^2 k_z^2}{\omega^2 k^2}, \tag{7}$$

where $\lambda_{D\alpha}(=\sqrt{k_B T_\alpha/4\pi n_\alpha q_\alpha^2})$ is the Debye length, $\delta \equiv \Delta n_+/n_+$, $\Delta n_+ = \Delta n_-$, and Δn_+ and Δn_- are, respectively, the density variations of positrons and electrons due to the electron-positron pair annihilations. Here, $\delta > 0$ and $\delta < 0$ represent the pair annihilations and creations, respectively. In this work, we only consider the direct positron annihilations with free electrons and the single photon annihilations of positrons with bound atomic electrons have been neglected since the one-photon positron annihilation cross section with an atomic electron is known to be quite small compared with the two-photon positron annihilation cross section with a free electron.[6,14] The plasma dielectric function for the ion cyclotron wave in magnetized electron-positron-ion plasmas including the direct electron-positron pair annihilations is then found to be

$$\varepsilon_l(\omega, k_x, k_z) \cong 1 + \frac{1}{k^2 \lambda_{D_-}^2}\left(1 - \frac{n_+}{n_-}\delta\right) + \frac{1}{k^2 \lambda_{D_+}^2}(1-\delta) - \frac{\omega_{pi}^2 k_x^2}{(\omega^2 - \omega_{ci}^2)k^2} - \frac{\omega_{pi}^2 k_z^2}{\omega^2 k^2}. \quad (8)$$

Very recently, the excellent discussions[15] on the physical properties of the nonlinear interaction effects involving the ion cyclotron waves were given in magnetoplasmas such as white dwarf and neutron star environments.

III. DISPERSION RELATION AND GROUP VELOCITY

From the mirror reflection condition for the electrostatic surface wave and the plasma dielectric function, the dispersion relation for the surface ion cyclotron wave is given by

$$\frac{1}{\pi}\int_{-\infty}^{\infty} \frac{dk_x\, k_z}{k_x^2 + k_z^2 + \frac{1}{\lambda_{D_-}^2}\left(1 - \frac{n_+}{n_-}\delta\right) + \frac{1}{\lambda_{D_+}^2}(1-\delta) - \frac{\omega_{pi}^2 k_x^2}{(\omega^2 - \omega_{ci}^2)} - \frac{\omega_{pi}^2 k_z^2}{\omega^2}} + 1 = 0. \quad (9)$$

Since $[(k_x^2 + k_z^2)\varepsilon_l(\omega, k_x, k_z)]^{-1} \to 0$ as $|k_x| \to \infty$, i.e., the Jordan's lemma,[16] the integration over k_x in the interval $[-\infty, \infty]$ in the spectral reflection condition would be replaced by the following contour integration in the complex k_x -plane:

$$\pi + \oint \frac{dk_x\, k_z}{k_x^2 + k_z^2 + \dfrac{1}{\lambda_{D_-}^2}\left(1 - \dfrac{n_+}{n_-}\delta\right) + \dfrac{1}{\lambda_{D_+}^2}(1-\delta) - \dfrac{\omega_{pi}^2 k_x^2}{(\omega^2 - \omega_{ci}^2)} - \dfrac{\omega_{pi}^2 k_z^2}{\omega^2}} = 0. \qquad (10)$$

By using the residue calculation for the simple pole in the upper-half plane in the complex k_x -plane, the dispersion relation for the surface ion cyclotron wave in magnetized electron-positron-ion plasmas in atmospheres of neutron stars is then obtained as

$$\omega^4 - (\omega_{ci}^2 + \omega_{pi}^2)\left[1 + \frac{k_z^2}{[1-(n_+/n_-)\delta]/\lambda_{D_-}^2 + (1-\delta)/\lambda_{D_+}^2}\right]\omega^2$$
$$+\omega_{ci}^2(\omega_{ci}^2 + \omega_{pi}^2)\frac{k_z^2}{[1-(n_+/n_-)\delta]/\lambda_{D_-}^2 + (1-\delta)/\lambda_{D_+}^2} = 0. \qquad (11)$$

The dependence of the density variation (δ) in equation (11) confirms the electron-positron pair annihilation effects on the propagation of the surface ion cyclotron wave in magnetized electron-positron-ion plasmas. From equation (11), the analytic solutions of the high (H) and low (L) frequency modes are, respectively, found to be as follows:

$$\left(\frac{\omega}{\omega_{pi}}\right)_H^2 = \frac{1}{2}\left\{\left[1+(\omega_{ci}/\omega_{pi})^2\right]\left[1+\frac{(k_z\lambda_{D\_})^2}{1+(n_+/n_-)(T_-/T_+)-(n_+/n_-)(1+T_-/T_+)\delta}\right]\right.$$

$$+\left[1+(\omega_{ci}/\omega_{pi})^2\right]^{1/2}\left[\left[1+\frac{(k_z\lambda_{D\_})^2}{1+(n_+/n_-)(T_-/T_+)-(n_+/n_-)(1+T_-/T_+)\delta}\right]^2\right.$$

$$\left.\left.+(\omega_{ci}/\omega_{pi})^2\left[1-\frac{(k_z\lambda_{D\_})^2}{1+(n_+/n_-)(T_-/T_+)-(n_+/n_-)(1+T_-/T_+)\delta}\right]^2\right]^{1/2}\right\},$$

(12)

$$\left(\frac{\omega}{\omega_{pi}}\right)_L^2 = \frac{1}{2}\left\{\left[1+(\omega_{ci}/\omega_{pi})^2\right]\left[1+\frac{(k_z\lambda_{D\_})^2}{1+(n_+/n_-)(T_-/T_+)-(n_+/n_-)(1+T_-/T_+)\delta}\right]\right.$$

$$-\left[1+(\omega_{ci}/\omega_{pi})^2\right]^{1/2}\left[\left[1+\frac{(k_z\lambda_{D\_})^2}{1+(n_+/n_-)(T_-/T_+)-(n_+/n_-)(1+T_-/T_+)\delta}\right]^2\right.$$

$$\left.\left.+(\omega_{ci}/\omega_{pi})^2\left[1-\frac{(k_z\lambda_{D\_})^2}{1+(n_+/n_-)(T_-/T_+)-(n_+/n_-)(1+T_-/T_+)\delta}\right]^2\right]^{1/2}\right\},$$

(13)

where T_- and T_+ are the temperatures of electrons and positrons, respectively. If we set $\Omega \equiv \omega_{ci}/\omega_{pi}$ and $K \equiv k_z\lambda_{D\_}/\left[1+(n_+/n_-)(T_-/T_+)-(n_+/n_-)(1+T_-/T_+)\delta\right]^{1/2}$, the high- and low-frequency mode solutions of the surface ion cyclotron wave in magnetized electron-positron-ion plasmas including the pair annihilation effects are represented by $(\omega/\omega_{pi})_{H,L} = \left\{(1+\Omega^2)(1+K^2)[1\pm\sqrt{F(\Omega,K)}]/2\right\}^{1/2}$, where H(L) corresponds to +(-) sign and $F(\Omega,K) \equiv [(1+K^2)^2+\Omega^2(1-K^2)^2]/[(1+\Omega^2)(1+K^2)^2]$. Here, $(\omega/\omega_{pi})_{H,L}^2 \geq 0$ since $F(\Omega,K) \leq 1$ for all values of *K*. Thus, the unstable growing mode of the ion cyclotron wave would be impossible in magnetized electron-positron-ion plasmas. We consider here the group velocity since the physical properties of the wave propagation can be analyzed by the group velocity of the wave. After some algebra, the group velocities for the high- and low- frequency modes are, respectively, given by

$$
\begin{aligned}
\frac{d(\omega/\omega_{pi})_H}{d(k_z\lambda_{D_-})} = \frac{1}{\sqrt{2}}\Bigg\{ & \left[1+(\omega_{ci}/\omega_{pi})^2\right]\frac{k_z\lambda_{D_-}}{1+(n_+/n_-)(T_-/T_+)-(n_+/n_-)(1+T_-/T_+)\delta} \\
& +\left[1+(\omega_{ci}/\omega_{pi})^2\right]^{1/2}\left[\left[1+\frac{(k_z\lambda_{D_-})^2}{1+(n_+/n_-)(T_-/T_+)-(n_+/n_-)(1+T_-/T_+)\delta}\right]\right. \\
& \left.-(\omega_{ci}/\omega_{pi})^2\left[1-\frac{(k_z\lambda_{D_-})^2}{1+(n_+/n_-)(T_-/T_+)-(n_+/n_-)(1+T_-/T_+)\delta}\right]\right]/ \\
& \left[\left[1+\frac{(k_z\lambda_{D_-})^2}{1+(n_+/n_-)(T_-/T_+)-(n_+/n_-)(1+T_-/T_+)\delta}\right]^2\right. \\
& \left.+(\omega_{ci}/\omega_{pi})^2\left[1-\frac{(k_z\lambda_{D_-})^2}{1+(n_+/n_-)(T_-/T_+)-(n_+/n_-)(1+T_-/T_+)\delta}\right]^2\right]^{1/2}\Bigg\}/ \\
& \Bigg\{\left[1+(\omega_{ci}/\omega_{pi})^2\right]\left[1+\frac{(k_z\lambda_{D_-})^2}{1+(n_+/n_-)(T_-/T_+)-(n_+/n_-)(1+T_-/T_+)\delta}\right] \\
& +\left[1+(\omega_{ci}/\omega_{pi})^2\right]^{1/2}\left[\left[1+\frac{(k_z\lambda_{D_-})^2}{1+(n_+/n_-)(T_-/T_+)-(n_+/n_-)(1+T_-/T_+)\delta}\right]^2\right. \\
& \left.+(\omega_{ci}/\omega_{pi})^2\left[1-\frac{(k_z\lambda_{D_-})^2}{1+(n_+/n_-)(T_-/T_+)-(n_+/n_-)(1+T_-/T_+)\delta}\right]^2\right]^{1/2}\Bigg\}^{1/2},
\end{aligned}
\tag{14}
$$

$$
\begin{aligned}
\frac{d(\omega/\omega_{pi})_L}{d(k_z\lambda_{D_-})} = \frac{1}{\sqrt{2}} \Bigg\{ & \left[1+(\omega_{ci}/\omega_{pi})^2\right] \frac{k_z\lambda_{D_-}}{1+(n_+/n_-)(T_-/T_+)-(n_+/n_-)(1+T_-/T_+)\delta} \\
& -\left[1+(\omega_{ci}/\omega_{pi})^2\right]^{1/2} \left[\left[1+\frac{(k_z\lambda_{D_-})^2}{1+(n_+/n_-)(T_-/T_+)-(n_+/n_-)(1+T_-/T_+)\delta}\right]\right. \\
& \left.-(\omega_{ci}/\omega_{pi})^2\left[1-\frac{(k_z\lambda_{D_-})^2}{1+(n_+/n_-)(T_-/T_+)-(n_+/n_-)(1+T_-/T_+)\delta}\right]\right] / \\
& \left[\left[1+\frac{(k_z\lambda_{D_-})^2}{1+(n_+/n_-)(T_-/T_+)-(n_+/n_-)(1+T_-/T_+)\delta}\right]^2\right. \\
& \left.+(\omega_{ci}/\omega_{pi})^2\left[1-\frac{(k_z\lambda_{D_-})^2}{1+(n_+/n_-)(T_-/T_+)-(n_+/n_-)(1+T_-/T_+)\delta}\right]^2\right]^{1/2} \Bigg\} / \\
& \Bigg\{ \left[1+(\omega_{ci}/\omega_{pi})^2\right]\left[1+\frac{(k_z\lambda_{D_-})^2}{1+(n_+/n_-)(T_-/T_+)-(n_+/n_-)(1+T_-/T_+)\delta}\right] \\
& -\left[1+(\omega_{ci}/\omega_{pi})^2\right]^{1/2} \left[\left[1+\frac{(k_z\lambda_{D_-})^2}{1+(n_+/n_-)(T_-/T_+)-(n_+/n_-)(1+T_-/T_+)\delta}\right]^2\right. \\
& \left.+(\omega_{ci}/\omega_{pi})^2\left[1-\frac{(k_z\lambda_{D_-})^2}{1+(n_+/n_-)(T_-/T_+)-(n_+/n_-)(1+T_-/T_+)\delta}\right]^2\right]^{1/2} \Bigg\}^{1/2} .
\end{aligned}
\tag{15}
$$

IV. PAIR ANNIHILATION EFFECTS

In order to investigate the effects of the electron-positron pair annihilation and the variations of the density and the temperature in the atmosphere of the neutron star on the wave frequencies and group velocities of surface ion cyclotron wave, we illustrate our results with numerical values of plasma parameters. The various physical properties of the high- and low- frequency mode waves can be investigated by equations (12) and (13). Figure 1 shows the three-dimensional plot of the high-frequency mode of ω/ω_{pi} as a function of the variation of the positron density $\Delta n_+/n_+(=\delta)$ and the scaled wave number $k_z\lambda_{D-}$ when $\omega_{ci}/\omega_{pi}=10$, $n_+/n_-=1$, and $T_-/T_+=1$. As we see in this figure, the wave frequency increases with the wave number. It is interesting to note that the electron-positron pair annihilation enhances the wave frequency in large wave number domains. Figure 2 shows the high-frequency mode of ω/ω_{pi} when $\omega_{ci}/\omega_{pi}=10$, $n_+/n_-=1$, and $T_-/T_+=10$. From Figures 2 and 1, we found that an increase of the electron temperature or a decrease of the positron temperature strongly suppresses the wave frequency. Thus, it is expected that the wave frequencies in high electron temperatures are smaller than those in low electron temperatures. Figure 3 represents the three-dimensional plot of the high-frequency mode of ω/ω_{pi} when $\omega_{ci}/\omega_{pi}=10$, $n_+/n_-=0.1$, and $T_-/T_+=1$. From Figures 3 and 1, a decrease of the electron density or an increase of the positron density weakens the electron-positron pair annihilation effects on the wave frequency. Figure 4 represents the high-frequency mode of ω/ω_{pi} when $\omega_{ci}/\omega_{pi}=1$, $n_+/n_-=1$, and $T_-/T_+=1$. From Figures 4 and 1, a decrease of the ion cyclotron frequency, i.e., a decrease of the magnetic field strength, strongly suppresses the wave frequency. Thus, the wave frequencies in atmospheres of neutron stars would be much smaller than those in atmospheres of magnetars due to the extremely strong magnetic field in magnetars. Figure 5 represents the three-dimensional plot of the low-frequency mode of ω/ω_{pi} as a function of the variation of the positron density $\Delta n_+/n_+$ and the scaled wave number

$k_z \lambda_{D_-}$ when $\omega_{ci} / \omega_{pi} = 10$, $n_+ / n_- = 1$, and $T_- / T_+ = 1$. As it is seen, the wave frequency has been saturated with increasing the wave number. Hence, we found that the low-frequency mode of the ion cyclotron wave cannot be propagated in large wave number domains in contrast to the high-frequency mode case. It is also found that the pair annihilation effects are negligible for the low-frequency mode case. Figure 6 represents the low-frequency mode of ω / ω_{pi} when $\omega_{ci} / \omega_{pi} = 10$, $n_+ / n_- = 1$, and $T_- / T_+ = 10$. From Figures 6 and 5, an increase of the electron temperature or a decrease of the positron temperature suppresses the increase of the wave frequency in small wave number domains, i.e., before approaching to the saturated oscillation frequency. Figure 7 shows the three-dimensional plot of the low-frequency mode of ω / ω_{pi} when $\omega_{ci} / \omega_{pi} = 10$, $n_+ / n_- = 0.1$, and $T_- / T_+ = 1$. From Figures 7 and 5, it is also found that the effects of the density variation on the wave frequency are negligible for the low-frequency mode case. Figure 8 shows the low-frequency mode of ω / ω_{pi} when $\omega_{ci} / \omega_{pi} = 1$, $n_+ / n_- = 1$, and $T_- / T_+ = 1$. From Figures 8 and 5, a decrease of the ion cyclotron frequency, i.e., a decrease of the magnetic field strength, strongly reduces the wave frequency such as in the case of the high-frequency mode. The physical properties of the group velocity for the high- and low- frequency modes would be investigated by equations (14) and (15). Figure 9 represents the group velocity $d(\omega / \omega_{pi}) / d(k_z \lambda_{D_-})$ for the high-frequency mode of the ion cyclotron wave as a function of the scaled wave number $k_z \lambda_{D_-}$ for various values of the variation of the positron density $\Delta n_+ / n_+$ when $\omega_{ci} / \omega_{pi} = 10$, $n_+ / n_- = 1$, and $T_- / T_+ = 1$. As it is seen, the group velocity has been suddenly increased for $k_z \lambda_{D_-} > 1$ and saturated in high wave number regions. It is also found that the pair annihilation strongly enhances the group velocity of the surface ion cyclotron wave for all values of the wave number. Figure 10 represents the group velocity for the high-frequency mode for various values of the temperature ratio T_- / T_+ when $\omega_{ci} / \omega_{pi} = 10$, $n_+ / n_- = 1$, and $\Delta n_+ / n_+ = 0.2$. From this figure, a decrease of the temperature ratio, i.e., a decrease of the electron temperature or an increase of the positron temperature, strongly enhances the group velocity. Figure

11 represents the group velocity for the high-frequency mode for various values of the frequency ratio ω_{ci}/ω_{pi} when $n_+/n_- = 1$, $T_-/T_+ = 1$, and $\Delta n_+/n_+ = 0.2$. It is shown that the group velocity increases with an increase of the frequency ratio ω_{ci}/ω_{pi}, i.e., an increase of the magnetic field strength, especially, for $k_z\lambda_{D_-} > 1$. However, for small wave number domains $(k_z\lambda_{D_-} < 1)$, an increases of the magnetic field suppresses the group velocity. Figure 12 shows the group velocity for the low-frequency mode for various values of the variation of the positron density $\Delta n_+/n_+$ when $\omega_{ci}/\omega_{pi} = 10$, $n_+/n_- = 1$, and $T_-/T_+ = 1$. In contrast to the case of the high-frequency mode, the group velocity for the low-frequency mode decreases with increasing the wave number. It should be noted that the electron-positron pair annihilation enhances the group velocity for $k_z\lambda_{D_-} < 1$ and, however, suppresses the group velocity for $k_z\lambda_{D_-} > 1$. From Figures 12 and 9, we can expect that the propagation of the ion cyclotron wave in electron-positron-ion plasmas such as in atmospheres of neurons stars is mainly determined by the low-frequency mode in small wave numbers $(k_z\lambda_{D_-} < 1)$ and the high-frequency mode in large wave numbers $(k_z\lambda_{D_-} > 1)$. Figure 13 shows the group velocity for the low-frequency mode for various values of the temperature ratio T_-/T_+ when $\omega_{ci}/\omega_{pi} = 10$, $n_+/n_- = 1$, and $\Delta n_+/n_+ = 0.2$. It is shown that an increase of the temperature ratio, i.e., an increase of the electron temperature or a decrease of the positron temperature, suppresses the group velocity for $k_z\lambda_{D_-} < 1$ and, however, enhances the group velocity for $k_z\lambda_{D_-} > 1$. Figure 14 shows the group velocity for the low-frequency mode for various values of the frequency ratio ω_{ci}/ω_{pi} when $n_+/n_- = 1$, $T_-/T_+ = 1$, and $\Delta n_+/n_+ = 0.2$. It is also shown that the group velocity significantly increases with an increase of the frequency ratio ω_{ci}/ω_{pi}, i.e., an increase of the magnetic field strength. However, for small wave numbers $(k_z\lambda_{D_-} < 1)$, the group velocity is suddenly decreased and the effect of the magnetic field strength is found to be small for large wave numbers $(k_z\lambda_{D_-} > 1)$.

V. CONCLUSIONS

In this work, we have investigated the electron-positron pair annihilation effects on the surface ion cyclotron wave in magnetized electron-positron-ion plasmas. The dispersion relation of the surface ion cyclotron wave is obtained by the specular reflection boundary condition with the dielectric susceptibilities for electrons, positrons, and ions. Considering the dispersion relation of the surface ion cyclotron wave, we observe that the high- and low-frequency modes of the surface ion cyclotron wave could be existed in electron-positron-ion plasmas. We have analyzed the effects of the pair annihilation on both high- and low-frequency modes of the surface ion cyclotron wave. The physical properties of the group velocity of the surface ion cyclotron wave are also discussed. In addition, we have investigated the effects of the temperature and magnetic field strength on the surface ion cyclotron wave. From this work, we have shown that the group velocities in atmospheres of magnetars would be much greater than those in atmospheres of normal neutron stars due to the extremely strong magnetic fields of magnetars. It is also shown that the propagation of the ion cyclotron wave in atmospheres of neurons stars is mainly determined by the low-frequency mode in small wave number regions and by the high-frequency mode in large wave number regions. Thus, we have found that the electron-positron pair annihilation plays an very significant role in the propagations of the surface wave in magnetized electron-positron-ion plasmas such as atmospheres of neutron stars.

ACKNOWLEDGMENTS

The authors gratefully acknowledge Professor L. Stenflo for providing us very valuable references. One of the authors (Y.-D.J.) gratefully acknowledges the Director-General Professor O. Motojima, Director Professor M. Sato, Director Professor Y. Hirooka, and Professor I. Murakami for warm hospitality while visiting the National Institute for Fusion Science (NIFS) in Japan as a long-term visiting professor. The authors are also grateful to NIFS for supporting the research. This work was done while Y.-D.J. visited NIFS.

REFERENCES

1) A. F. Alexandrov, L. S. Bogdankevich, and A. A. Rukhadze, *Principles of Plasma Electrodynamics* (Springer, Berlin, 1984).
2) L. Stenflo, *Phys. Scripta* **T63**, 59 (1996).
3) H. J. Lee and H. S. Hong, Phys. Plasmas **5**, 4094 (1998).
4) T. Tajima aand K. Shibata, *Plasma Astrophysics* (Addison Wesley, Reading, 2002).
5) V. B. Berestetskii, E. M. Lifshitz, and L. P. Pitaevskii, *Quantum Electrodynamics*, 2nd ed. (Pergamon, Oxford, 1982).
6) Y.-D. Jung*, Astrophys. J.* **424**, 988 (1994).
7) P. K. Shukla, *Europhys. Lett.* **22**, 695 (1993).
8) S.-H. Cho, H. J. Lee, and Y.-S. Kim, *Phys. Rev. E* **61**, 4357 (2000).
9) P. K. Shukla, and M. Marklund, *Phys. Scr*. **T113**, 36 (2004).
10) S. Ali, W. M. Moslem, P. K. Shukla, and R. Schlickeiser, *Phys. Plasmas* **14**, 082307 (2007).
11) N. Shukla, P. K. Shukla, and G. E. Morfill, *J. Plasma Phys.* **73**, 289 (2007).
12) M. Tribeche, L. A. Gougam,N. Boubakour, and T. H. Zerguini, *J. Plasma Phys.* **73**, 403 (2007).
13) P. K. Shukla and A. A. Mamun, *Introduction to Dusty Plasma Physics* (Institute of Physics Publishing, Bristol, 2002)
14) E. Fermi and G. E. Uhlenbeck, *Phys. Rev.* **44**, 510 (1933)
15) P. K. Shukla, S. Ali, L. Stenflo, and M. Marklund, *Phys. Plasmas* **13**, 112111(2006)
16) J. Mathews and R. L. Walker, *Mathematical Methods of Physics*, 2nd ed. (Benjamin, New York, 1970)

FIG. 1. The three-dimensional plot of the high-frequency mode of ω / ω_{pi} as a function of $\Delta n_+ / n_+$ and $k_z \lambda_{D_-}$ when $\omega_{ci} / \omega_{pi} = 10$, $n_+ / n_- = 1$, and $T_- / T_+ = 1$.

Figure 1

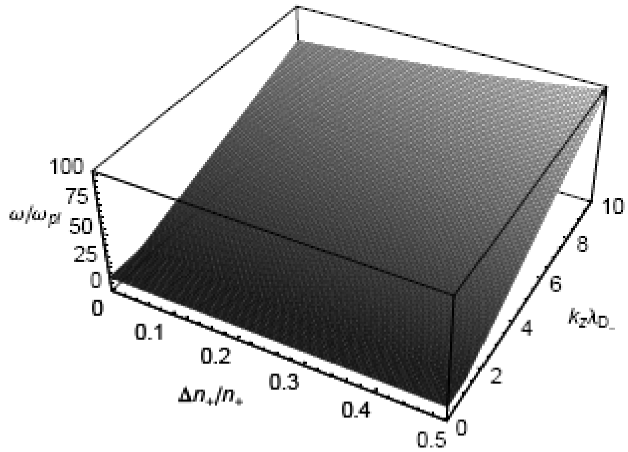

FIG. 2. Same as Fig. 1, but for $T_- / T_+ = 10$.

Figure 2

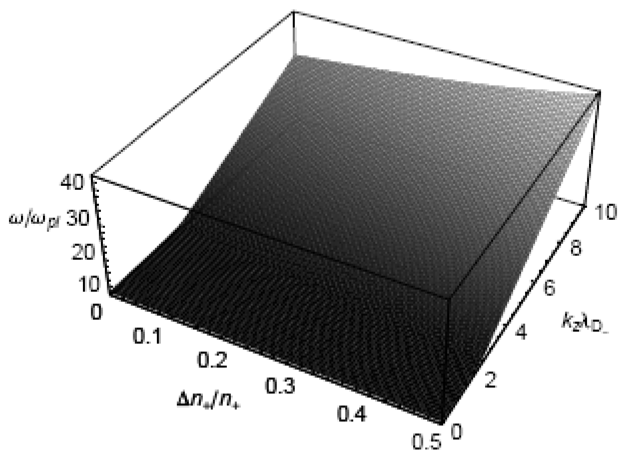

FIG. 3. Same as Fig. 1, but for $n_+ / n_- = 0.1$.

Figure 3

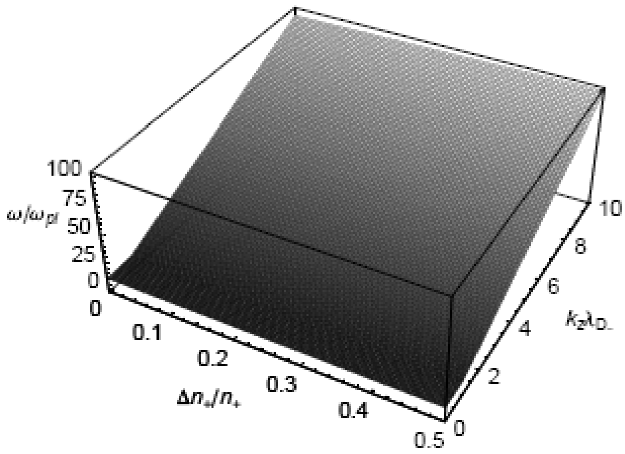

FIG. 4. Same as Fig. 1, but for $\omega_{ci} / \omega_{pi} = 1$.

Figure 4

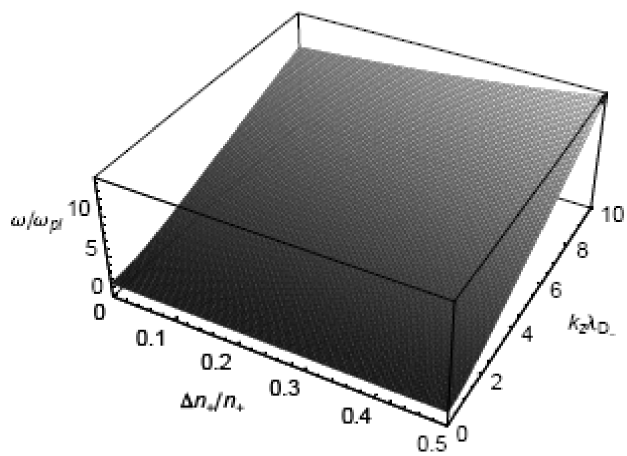

FIG. 5. The three-dimensional plot of the low-frequency mode of ω/ω_{pi} as a function of $\Delta n_+/n_+$ and $k_z\lambda_{D_-}$ when $\omega_{ci}/\omega_{pi}=10$, $n_+/n_-=1$, and $T_-/T_+=1$.

Figure 5

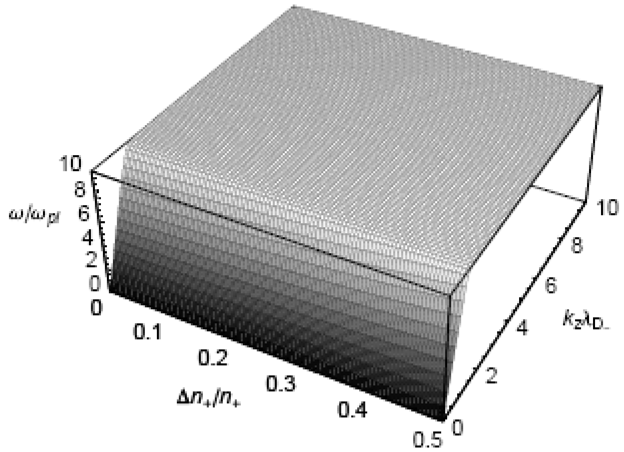

FIG. 6. Same as Fig. 5, but for $T_-/T_+=10$.

Figure 6

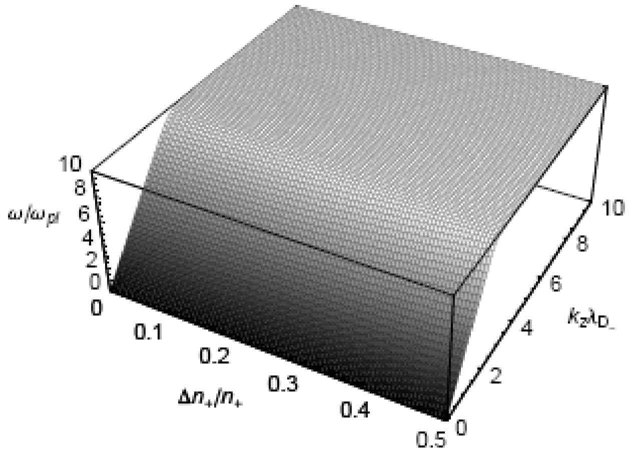

FIG. 7. Same as Fig. 5, but for $n_+ / n_- = 0.1$.

Figure 7

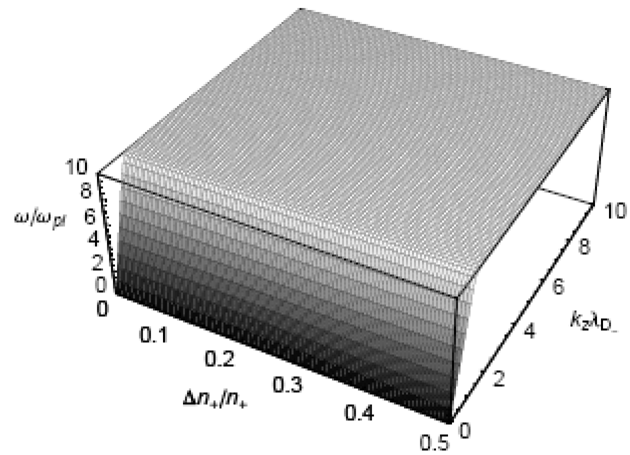

FIG. 8.—Same as Fig. 5, but for $\omega_{ci} / \omega_{pi} = 1$.

Figure 8

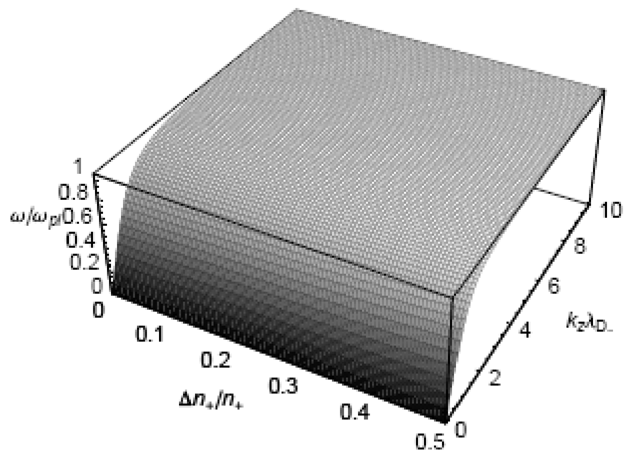

FIG. 9. The group velocity $d(\omega/\omega_{pi})/d(k_z\lambda_{D_-})$ for the high-frequency mode as a function of $k_z\lambda_{D_-}$ when $\omega_{ci}/\omega_{pi}=10$, $n_+/n_-=1$, and $T_-/T_+=1$. The solid line represents the case of $\Delta n_+/n_+=0.1$. The dashed line represents the case of $\Delta n_+/n_+=0.3$. The dotted line represents the case of $\Delta n_+/n_+=0.6$.

Figure 9

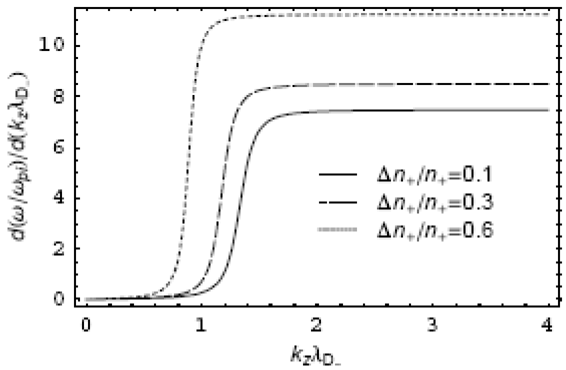

FIG. 10. The group velocity $d(\omega/\omega_{pi})/d(k_z\lambda_{D_-})$ for the high-frequency mode as a function of $k_z\lambda_{D_-}$ when $\omega_{ci}/\omega_{pi}=10$, $n_+/n_-=1$, and $\Delta n_+/n_+=0.2$. The solid line represents the case of $T_-/T_+=0.5$. The dashed line represents the case of $T_-/T_+=1$. The dotted line represents the case of $T_-/T_+=2$.

Figure 10

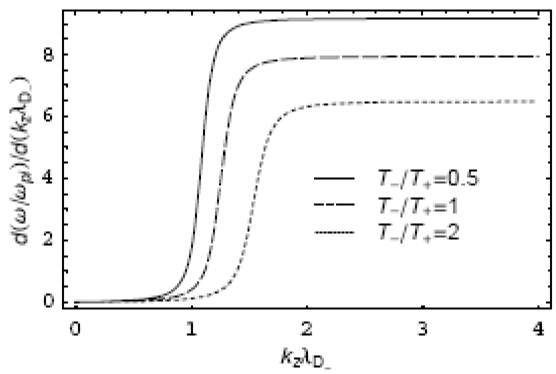

FIG. 11. The group velocity $d(\omega/\omega_{pi})/d(k_z\lambda_{D_-})$ for the high-frequency mode as a function of $k_z\lambda_{D_-}$ when $n_+/n_-=1$, $T_-/T_+=1$, and $\Delta n_+/n_+=0.2$. The solid line represents the case of $\omega_{ci}/\omega_{pi}=20$. The dashed line represents the case of $\omega_{ci}/\omega_{pi}=10$. The dotted line represents the case of $\omega_{ci}/\omega_{pi}=1$.

Figure 11

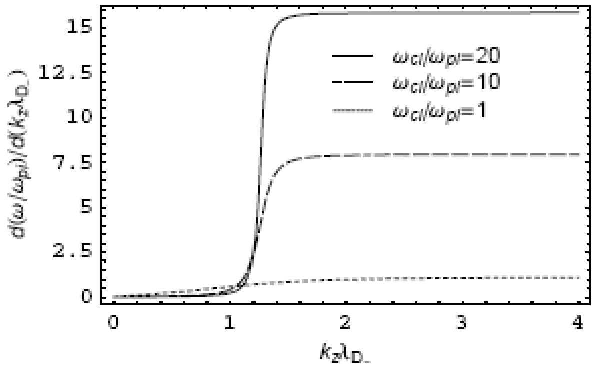

FIG. 12. The group velocity $d(\omega/\omega_{pi})/d(k_z\lambda_{D_-})$ for the low-frequency mode as a function of $k_z\lambda_{D_-}$ when $\omega_{ci}/\omega_{pi}=10$, $n_+/n_-=1$, and $T_-/T_+=1$. The solid line represents the case of $\Delta n_+/n_+=0.1$. The dashed line represents the case of $\Delta n_+/n_+=0.3$. The dotted line represents the case of $\Delta n_+/n_+=0.6$.

Figure 12

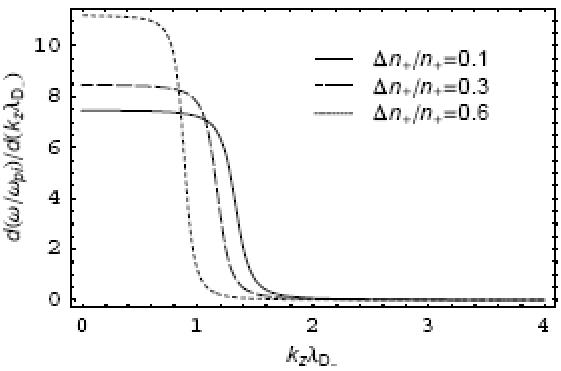

FIG. 13. The group velocity $d(\omega/\omega_{pi})/d(k_z\lambda_{D\_})$ for the low-frequency mode as a function of $k_z\lambda_{D\_}$ when $\omega_{ci}/\omega_{pi}=10$, $n_+/n_-=1$, and $\Delta n_+/n_+=0.2$. The solid line represents the case of $T_-/T_+=0.5$. The dashed line represents the case of $T_-/T_+=1$. The dotted line represents the case of $T_-/T_+=2$.

Figure 13

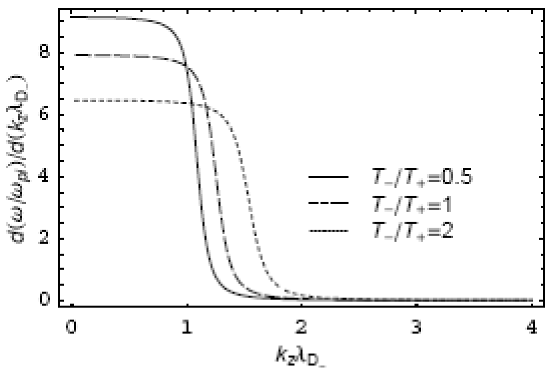

FIG. 14. The group velocity $d(\omega/\omega_{pi})/d(k_z\lambda_{D\_})$ for the low-frequency mode as a function of $k_z\lambda_{D\_}$ when $n_+/n_-=1$, $T_-/T_+=1$, and $\Delta n_+/n_+=0.2$. The solid line represents the case of $\omega_{ci}/\omega_{pi}=20$. The dashed line represents the case of $\omega_{ci}/\omega_{pi}=10$. The dotted line represents the case of $\omega_{ci}/\omega_{pi}=1$.

Figure 14